Oxidation of diclofenac by birnessite: Identification of products and proposed transformation pathway

Yue Zhao [1,2], Fei Liu [2,*], Min Wang [1,*], Xiaopeng Qin [3]

[1] Institute of Quality Standards and Testing Technology for Agro-Products, Key Laboratory of Agro-Product Quality and Safety, Chinese Academy of Agricultural Sciences, Beijing 100081, China
[2] School of Water Resources and Environment, and Beijing Key Laboratory of Water Resources and Environmental Engineering, China University of Geosciences (Beijing), Beijing 100083, China
[3] Department of Technology Assessment, Technical Centre for Soil, Agricultural and Rural Ecology and Environment, Ministry of Ecology and Environment, Beijing 100012, China

ARTICLE INFO

ABSTRACT

Diclofenac (DCF), a widely used non-steroidal anti-inflammatory, reacted readily with birnessite under mild conditions, and the pseudo first order kinetic constants achieved 8.84×10^{-2} hr^{-1}. Five products of DCF including an iminoquinone product (2,5-iminoquinone-diclofenac) and four dimer products were observed and identified by tandem mass spectrometry during the reaction. Meanwhile, 2,5-iminoquinone-diclofenac was identified to be the major product, accounting for 83.09% of the transformed DCF. According to the results of spectroscopic Mn(III) trapping experiments and X-ray Photoelectron Spectroscopy, Mn(IV) contained in birnessite solid was consumed and mainly converted into Mn(III) during reaction process, which proved that the removal of DCF by birnessite was through oxidation. Based on the identified products of DCF and the changes of Mn valence state in birnessite solid, a tentative transformation pathway of DCF was proposed.

© 2020 The Research Center for Eco-Environmental Sciences, Chinese Academy of Sciences. Published by Elsevier B.V.

Introduction

Diclofenac (DCF), a novel non-steroidal anti-inflammatory, is widely used clinically for the treatment of pain and inflammation for human and animals. Due to its annual large global consumption (about 1443±58 tons) (Acuña et al., 2015) and low removal efficiency in wastewater treatment plants (about 2%-60%) (Wang and Wang, 2016), it has been frequently detected in surface water, groundwater, soils, and sediments (Duan et al., 2013; Lindholm-Lehto et al., 2015; Simazaki et al., 2015; Meyer et al., 2016; Biel-Maeso et al., 2017, 2018). DCF accumulates in the organisms through food chain, posing great threat to their health. For example, it caused vulture deaths on a large scale in Indian subcontinent in 1990s (Oaks et al., 2004). Moreover, ulcers and bleeding in gastric glandular induced by DCF was also documented (El-Deen et al., 2016). It has been added to watch list of "EU Water Framework Directive" since 2013. Accordingly, the environmental fate of DCF has drawn much attention worldwide.

Adsorption and oxidation of pharmaceuticals and personal care products (PPCPs) were major process affecting their ultimate fate in the environment. Previous literature showed that the storage and degradation of DCF were 5.51% and 93.11% respectively in surface 90 cm of the loamy sand soil profile following a 10 years simulation of turf grass irrigation using reclaimed water (Chen et al., 2013). Xu et al. (2009) reported that the half-lives of DCF in four agricultural soils were varied from 3.07 to 20.44 days un-

* Corresponding authors.
  E-mails: feiliu@cugb.edu.cn (F. Liu), wangmin@caas.cn (M. Wang).

der the aerobic condition. It was well known that the presence of PPCPs (*i.e.* paracetamol, ibuprofen, diclofenac, and cefazolin) in environment exerted adverse effects on organisms (Chen et al., 2017; Yang et al., 2017; Rede et al., 2019). In fact, some transformation products exhibited greater toxicity than their parent compounds (Li et al., 2017; Lu et al., 2017). These features necessitated researchers to understand the actual fate and dissipation of PPCPs in environment. Therefore, it was not enough to just focus on the removal efficiency of DCF from soil environment.

Metal oxides are abundantly present in soils/sediments and play important roles in removal of PPCPs through adsorption and/or redox reaction. Manganese oxides (MnO_x), as important natural catalysts and oxidants, have been found to significantly affect the environmental fate and transformation of organic pollutants (Lu et al., 2011; Qin et al., 2016). Previous studies showed that birnessite as the most ubiquitous type of $MnO_x(s)$ could react with various types of PPCPs, such as rhodamine B (Qin et al., 2016), *p*-arsanilic acid (Wang and Cheng, 2015), and so on. In our previous study, we also found that DCF was easily and efficiently removed by birnessite (Zhao et al., 2019). In fact, DCF adsorbed on the surface of birnessite and formed a complexation precursor firstly, then, fast electron transfer occurred within the precursor. However, it is not clear the fate and potential risk of DCF attenuation by birnessite in environment. Figuring out the attenuation mechanism and transformation products of DCF reacted with birnessite will be helpful to understand the environmental fate of DCF deeply and determine risk reduction measures.

This study aims to reveal the transformation process of DCF with birnessite in aqueous solution. Ultra-performance Liquid Chromatography Triple Quadrupole Mass Spectrometry (UPLC-MS/MS), Fourier Transform Infrared Spectroscopy (FT-IR) and X-ray Photoelectron Spectroscopy (XPS) measurements were utilized to analyze transformation products of DCF and changes of birnessite during reaction process. Based on the above, tentative transformation pathways of DCF by birnessite were proposed.

1. Materials and methods

1.1. Materials

Diclofenac sodium (>98%), oxalic acid and 5-hydroxydiclofenac (>98%) were purchased from Sigma-Aldrich (USA). Methanol (HPLC grade) was acquired from Honeywell Burdick & Jackson (USA). Birnessite was synthesized in our laboratory, using the procedure developed by McKenzie (1971) as described in our previous work (Zhao et al., 2019). Pyrophosphate sodium was produced by Sinopharm Chemical Reagent Co., Ltd. (Shanghai, China). Manganese dioxide was provided by Xilong Scientific (Shantou, China). H_2SO_4 (98%) was acquired from Beijing Chemical Works (Beijing, China). $MnCl_2 \cdot 4H_2O$ (≥99%) was obtained from Fuchen Chemical Reagents Factory (Tianjin, China). All chemicals were analytical reagent or higher and all solutions were prepared using the ultrapure water (MILLI-Q, USA).

1.2. Batch experiment

The experiments were carried out in 40 mL amber sample vials. In present experiments, high concentration of DCF (10 mg/L) and birnessite (1 g/L) were adopted in order to ensure capture more transformation products. The pH of suspensions was adjusted by adding 0.01 mol/L HCl or 0.01 mol/L NaOH. Then, the mixture of DCF and birnessite was placed in a reciprocal shaker operated at 175 r/min and 25 °C in the dark. Samples were withdrawn at specific time intervals varied from 0 hr to 96 hr and centrifuged at 3000 r/min for 10 min. The supernatants were used to analyze the changes of DCF, products of DCF, total organic carbon (TOC) and chlorine anions in system. All experiments were conducted in triplicates. The final pH of each sample was measured using a pH meter (Sartorius PB-10, Germany). Meanwhile, blank samples (only containing birnessite) and control samples (only containing DCF) were also carried out.

1.3. Spectroscopic Mn(III) trapping experiment

The samples were prepared using identical method as mentioned in Section 1.2. After centrifugation, the supernatants were taken out totally and used to analyze the concentration of Mn(II) in system by Inductively Coupled Plasma Optical Emission Spectrometer (ICP-OES) (SPECTROBLUE, Germany). The residual solids in bottles were treated by 20 mL sodium pyrophosphate solution (50 mol/L, pH = 7) in order to analyze the concentration of Mn(III) (Klewicki and Morgan, 1998; Webb et al., 2005). After shaking in a reciprocal shaker (175 r/min, 25 °C) for 24 hr, the samples were filtered and stored at 4 °C in the dark prior to analysis. The concentration of Mn(III) in these samples was determined using UV-Visible Spectrophotometer (Shimadzu UV-1800, Japan). Details about the determination method were given in **Appendix A Text S1**.

1.4. Average oxidation state of Mn

The average oxidation state (AOS) of Mn was measured using oxalic acid oxidation method (Kijima et al., 2001; Zhao et al., 2009). Firstly, 20 mg of birnessite solid was dissolved in 20 mL of hydrochloric acid hydroxylamine (0.25 mol/L) and the total content of Mn was measured by ICP-OES. Secondly, birnessite solids at various reaction time intervals were completely dissolved in 5 mL $H_2C_2O_4$ (0.5 mol/L) and 10 mL H_2SO_4 (1 mol/L) to reduce manganese ions with highly valence state to Mn(II). Then the samples were diluted and residual $C_2O_4^{2-}$ was analyzed using High Performance Liquid Chromatography (HPLC) (Shimadzu LC-20AT, Japan). The AOS of Mn was calculated using the follow equation:

$$AOS = 2 \cdot \left(N_{C_2O_4^{2-}} \cdot V \cdot M/m \cdot C + 1 \right) \qquad (1)$$

where $N_{C_2O_4^{2-}}$ (N) is the equivalent concentration of oxalic acid in the reaction; V (L) is the volume of aqueous phase; M (g/mol) is the molar mass of manganese, 54.938 g/mol; m (g) is the mass of birnessite solid; C (%) is the mass fraction of total Mn in birnessite.

1.5. Characterization of birnessite

Samples for FT-IR analysis were carried out with initial DCF concentration ranged from 0 to 50 mg/L in system. Solids were separated by centrifugation and dried using a freeze drier (LGJ-10D, China) after shaking for 72 hr. The dried samples were mixed with KBr power (sample: KBr $\approx$1: 50) and pressed to pellets for testing. The infrared spectra of samples were acquired using a FT-IR spectrometer (Gang-dong FTIR-650, China), operating in the mid-infrared range between 400 and 4000 cm^{-1} with 16 scans at a resolution of 4 cm^{-1}.

Samples for X-ray Photoelectron Spectroscopy (XPS) analysis were taken from three batch experiments which reaction times were set to 0, 12, and 72 hr respectively. The spectra of samples were collected using a XPS (Thermo Fisher Scientific Escalab 250Xi, USA) with a resolution of 0.05 eV. The reference binding energy used adventitious carbon contamination (C1s = 284.6 eV). The narrow-area XPS pattern of element was subjected to multi-peak Gauss-Lorentz fitting to separate overlapping peaks using XPSpeak 41 software.

1.6. HPLC and mass spectral analysis

The concentration of oxalic acid in solution was determined by HPLC equipped with an InertSustainSwift C18 column (4.6 mm × 250 mm, 5 μm particle size). The mobile phase was consisted of 2% methanol and 98% phosphate (0.01 mol/L, pH 2.5). The flow rate was 0.8 mL/min. 10 μL of sample was injected using an auto-sampling device, with the detection wavelength set to 210 nm. The column temperature was kept at 35 °C.

The concentration of DCF in solutions was determined by HPLC as described in our previous work (Zhao et al., 2017). Transformation products of DCF were identified using Ultra-high Performance Liquid Chromatography coupled to Triple Quadrupole Mass Spectrometry (UPLC-QqQ-MS/MS), equipped with Electrospray Ion Source (ESI) (Waters Xevo TQ-S, USA). The details of elution program and MS parameters were given in **Appendix A Text S2**.

2. Results and discussion

2.1. Kinetic process of DCF transformation by birnessite

In absence of birnessite, DCF was remained intact in aqueous solution, and its concentration did not markedly decrease under the experimental conditions (data not shown). However, in presence of birnessite, the decreased of DCF concentration depended on the treatment period. As shown in Fig. 1, DCF was almost totally removed by birnessite after 72 hr. The kinetic curve followed pseudo first order kinetic (R^2 > 0.97), and the pseudo first order kinetic rate constant of DCF was 8.84 × 10^{-2} hr^{-1} **(Appendix A Table S1)**. It was worth noting that the formation of five transformation products (P1-P5) of DCF was observed in system **(Appendix A Fig. S2)**. Meanwhile, TOC in the system was not significantly reduced with increasing reaction time **(Fig. 1a)**. The removal efficiency of TOC was just 4.15% at 96 hr, but DCF was totally removed at this moment. In addition, Cl$^-$ was not found in the reaction system
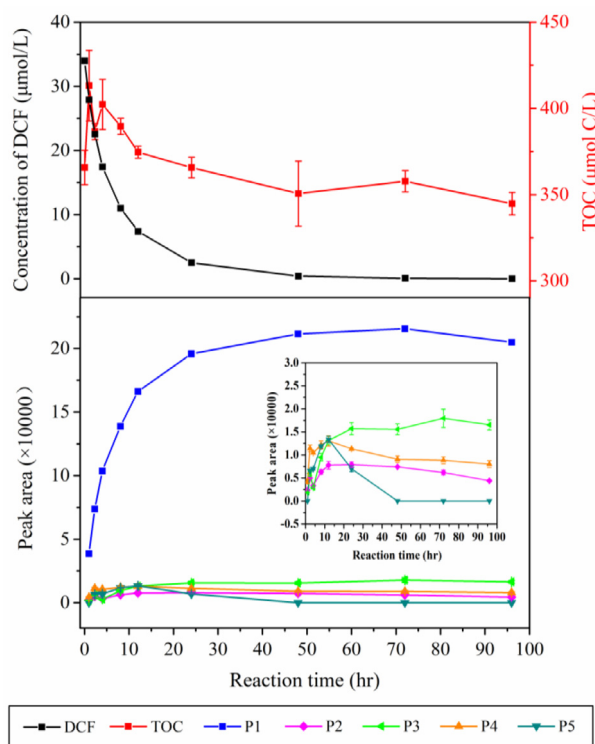

Fig. 1 – Typical time courses of DCF transformation by birnessite. Error bars (±1 standard deviation, *n* = 3) are shown in the figures. The intial concentration of DCF is 10 mg/L. The concnentraion of birnessite is 1 g/L. The solution pH is 7.23 ± 0.05.

(data not shown). It was indicated that the removal of DCF by birnessite was chemical conversion and mineralization of DCF was unlikely. Similarly, DCF also could not be mineralized by permanganate (Cheng et al., 2015).

As shown in Fig. 1, the products P1 and P3 increased quickly with increasing reaction time (0-24 hr) and then reached apparent equilibrium at 48 hr. Nevertheless, P2, P4 and P5 increased with increasing reaction time firstly and reached their maximum at 12 hr. Then P2 and P4 decreased slowly with increasing reaction time (12-96 hr). Meanwhile, P5 decreased quickly after 12 hr and was not detected in the system at 48 hr. It was suggested that P1 and P3 possessed excellent chemical stability in the system. Furthermore, the peak area of P1 was always the highest during reaction progress, and was an order magnitude higher than that of other products (P2-P5) at 96 hr. Furthermore, the kinetic formation curve of P1 was well agreed with the attenuation curve of DCF. When the concentration of DCF achieved the smallest value (72 hr), the maximum peak area value of P1 was observed. The product P1 was not only detected in system with high initial DCF concentration (10 mg/L), but also in that with low initial DCF concentration (0.25 mg/L). However, other products, such as P2 to P5, were not observed in low initial DCF concentration system (data not shown). These observations suggest that P1 was the major product of DCF. Assuming that P1 possessed identical UV response as DCF, it would represent 83.09% of the transformed DCF (10 mg/L).
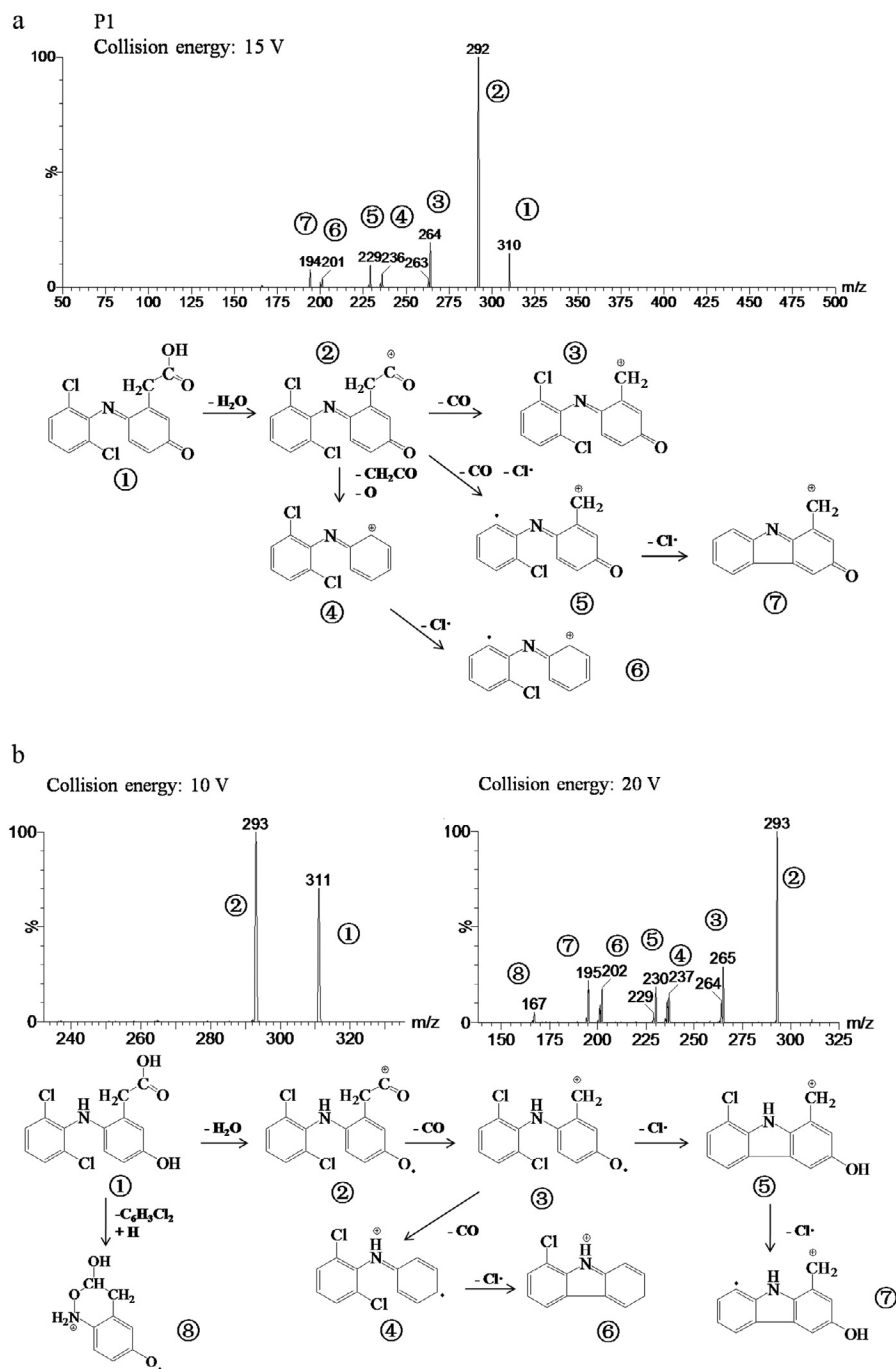
Fig. 2 – MS spectra and proposed fragmentation pathways of P1 (*m/z* 310) (a) and intermediate product (*m/z* 311) (b).

2.2. Identification products of DCF

2.2.1. Mass spectrometry analysis of major product

P1 presented the molecular ion peak at *m/z* 310 which increased by 14 Da compared to that of DCF. And the molecular ion peak of P1 shown the isotopic distribution at M/M+2/M+4 (9:6:1), indicating that P1 possessed two chlorine atoms in structure. As shown in Fig. 2a, several fragmentations corresponding to Cl, H_2O, and carboxylic acid function group eliminations were observed, and the fragmentation pattern of P1 was proposed. Moreover, P1 displayed two strong UV adsorp-

tion wavelengths at 200 nm and 266 nm. Due to mass difference of +14 compared to DCF, the presence of chlorine atoms and the features of UV absorption wavelength, 2,5-iminoquinone-diclofenac (2,5-IQ-DCF) was suggested for P1. According to previous literatures, 2,5-IQ-DCF was also formed in the system that DCF oxidized by other manganese oxides (*i.e.* bio-manganese oxide and permanganate) (Forrez et al., 2010; Cheng et al., 2015).

In current study, the characteristic fragment ion peaks of hydroxydiclofenac product, such as *m/z* 311 and *m/z* 293, were also observed (Fig. 2b). The detection of fragment *m/z*

167 supported that a complete dichlorobenzene moiety was removed from fragment m/z 311. It was suggested that hydroxylation process occurred at C5 position of DCF. And 5-hydroxydiclofenac (5-OH-DCF) might be formed in the reaction between DCF and birnessite. This was confirmed using 5-OH-DCF standard, *i.e.* the pattern of the m/z ratios of fragment ions was identical. And the retention time of standard by HPLC analysis was also identical. Commonly, hydroxylation of DCF was the first step to form a product with quinine structure (Chong et al., 2017).

The detection of 5-OH-DCF in the reaction between DCF and birnessite further confirmed that P1 was 2,5-IQ-DCF. The first step in the attenuation of DCF by birnessite was hydroxylation of phenylethanoic acid ring at the para position of nitrogen atom. The formed 5-OH-DCF was unstable under oxidation environment, then it was further dehydrogenated to form 2,5-IQ-DCF (Groning et al., 2007; Lu et al., 2017). In the presence of manganese oxides, 5-OH-DCF was rapidly (less than 15 min) converted to 2,5-IQ-DCF (Forrez et al., 2010). Therefore, the change curve of 5-OH-DCF with reaction time was not observed in current study.

2.2.2. *Mass spectrometry analysis of minor dimer products*

It is well known that an even number of nitrogen atoms corresponds with an even molecular weight. As shown in Fig. 3, these products presented the molecular ion peak at m/z 659, 533, 607 and 631 in positive mode, suggesting that an even number of nitrogen atoms existed in the structures. In addition, they possessed 4 chlorine atoms in their structures according to isotopic distribution of chlorine atoms in MS spectra. Therefore, these products P2-P5 might be dimers. Dimer products were detected in oxidation of DCF by ozone or photodegradation of DCF under natural sunlight (Agüera et al., 2005; Sein et al., 2008). The formation of dimer products also observed in the transformation of DCF by natural manganese oxides (79% MnO_2) in the column experiment, and their molecular ions exact mass ranged from 511 to 548 (Huguet et al., 2013).

As can be seen, the MS/MS spectrum of P2 showed a few fragment ion peaks, and the fragment m/z 348 was the most obvious one. It was indicated that there were two intact fragments m/z 348 and m/z 311 existed in P2 structure. Furthermore, the fragments m/z 615 (loss of COO from fragment m/z 659), m/z 571 (loss of COO from fragment m/z 615), and m/z 535 (loss of two H_2O from fragment m/z 571) were observed (Fig. 3 and **Appendix A Fig. S3**), suggesting that P2 possessed two carboxyl function groups and hydroxyl function groups at least in structure. The fragment m/z 438 indicated the loss of $C_6H_4NCl_2O$ from m/z 615 (**Appendix A Fig. S3**), which suggested the hydroxylation of 2,6-dichloroaniline moiety in DCF occurred during the oxidation process.

In the MS/MS spectrum of P3, the fragments m/z 496, 426 and 392 generated by the loss of Cl function group were observed, which supported that P3 possessed four chlorine atoms in the structure. Meanwhile, the loss of OH function group (m/z 515) from P3 was also observed (**Appendix A Fig. S4**). It was noting that the loss of a carboxyl function group was not detected in MS fragmentation, suggesting that P3 did not possess carboxyl function group in the structure. Byproduct 2.5-IQ-DCF could be further decarboxylated in presence of

manganese oxides and transformed to some different unstable decarboxylated intermediates (Huguet et al., 2013). The observation of fragments m/z 340 and 249 indicated that dimer P3 was formed by coupling of the intermediates in decarboxylation process of DCF.

In the MS/MS spectrum of P4, the observation of fragment ion peaks m/z 589 and 561 supported that hydroxyl and carboxyl function group existed in P4 structure. And the fragment m/z 444 attributed to the loss of dichloroaniline structure from P4 was observed, indicating P4 possessed dichloroaniline moiety in the structure. Both of the fragment m/z 294 and 264 contained two chlorine atoms in their structure according to the chlorine isotopic distribution, suggesting they maintained dichloroaniline structure. These observations indicated that a chemical skeleton similar to DCF was possibly stayed intact in dimer P4. The most probable elemental composition of m/z 294 was proposed to be $C_{14}H_{11}Cl_2NO_2$. And the elemental composition of residual part of P4 (expect for the fragment m/z 294) was $C_{14}H_{11}Cl_2NO_3$, indicating that hydroxydiclofenac product involved in the dimerization reaction to form P4. This was also supported by the observation of fragment m/z 264 in MS/MS spectrum of P4.

Compared with the mass spectrum of P2-P4, the fragment ion peaks observed in the mass spectrum of P5 exhibited segmented characteristic distinctly and focused on m/z 50-100, 180-354 and 569-632 (Fig. 3 and **Appendix A Fig. S6**). The characteristic mass losses like 18 Da (-H_2O), 44 Da (-COO) and 36 Da (HCl) were observed from the MS/MS spectra of P5, supporting that hydroxyl and carboxyl function group existed in P5 structure. It was noting that only fragment m/z 75 was observed in the low mass charge ration (m/z 50-100) of MS/MS spectra of P5 under different collision energy (5-25 V). When the collision energy of mass spectrometry was set to 5 V, the chemical structure of P5 might be not broken totally due to the presence of a few fragment ion peaks in MS/MS spectrum. Therefore, an intact moiety m/z 75 which most likely possessed a five-membered heterocyclic ring structure existed in the P5 chemical structure.

Considering the observation information above, the most probable elemental composition of products and the information on transformation products from former DCF oxidation processes, *i.e.* chlorination, manganese oxides oxidation, and ozonization (Agüera et al., 2005; Sein et al., 2008; Huguet et al., 2013; Cheng et al., 2015; Wang et al. 2015), the proposed molecular structure of detected dimers in the current study were shown in Fig. 3. And the most probable elemental compositions of these products were proposed to be $C_{28}H_{24}Cl_4N_2O_8$ (P2), $C_{26}H_{18}Cl_4N_2O_2$ (P3), $C_{28}H_{20}Cl_4N_2O_7$ (P4) and $C_{27}H_{24}Cl_4N_2O_7$ (P5).

2.3. *Interaction mechanisms*

2.3.1. *Proof of interface reaction by FT-IR*

FT-IR spectroscopy was used to analyze the changes on birnesstie solid after reacting with DCF (Fig. 4). For non-reacted birnessite (Fig. 4a), the broad band at 3399 cm^{-1} corresponded with the stretching vibration of absorbed H_2O, and the band at 1631 cm^{-1} was assigned to the H-O-H bending vibration of surface or interlayer water. A strong intensity bands at 503 and 436 cm^{-1} were assigned to the stretching vibrations of
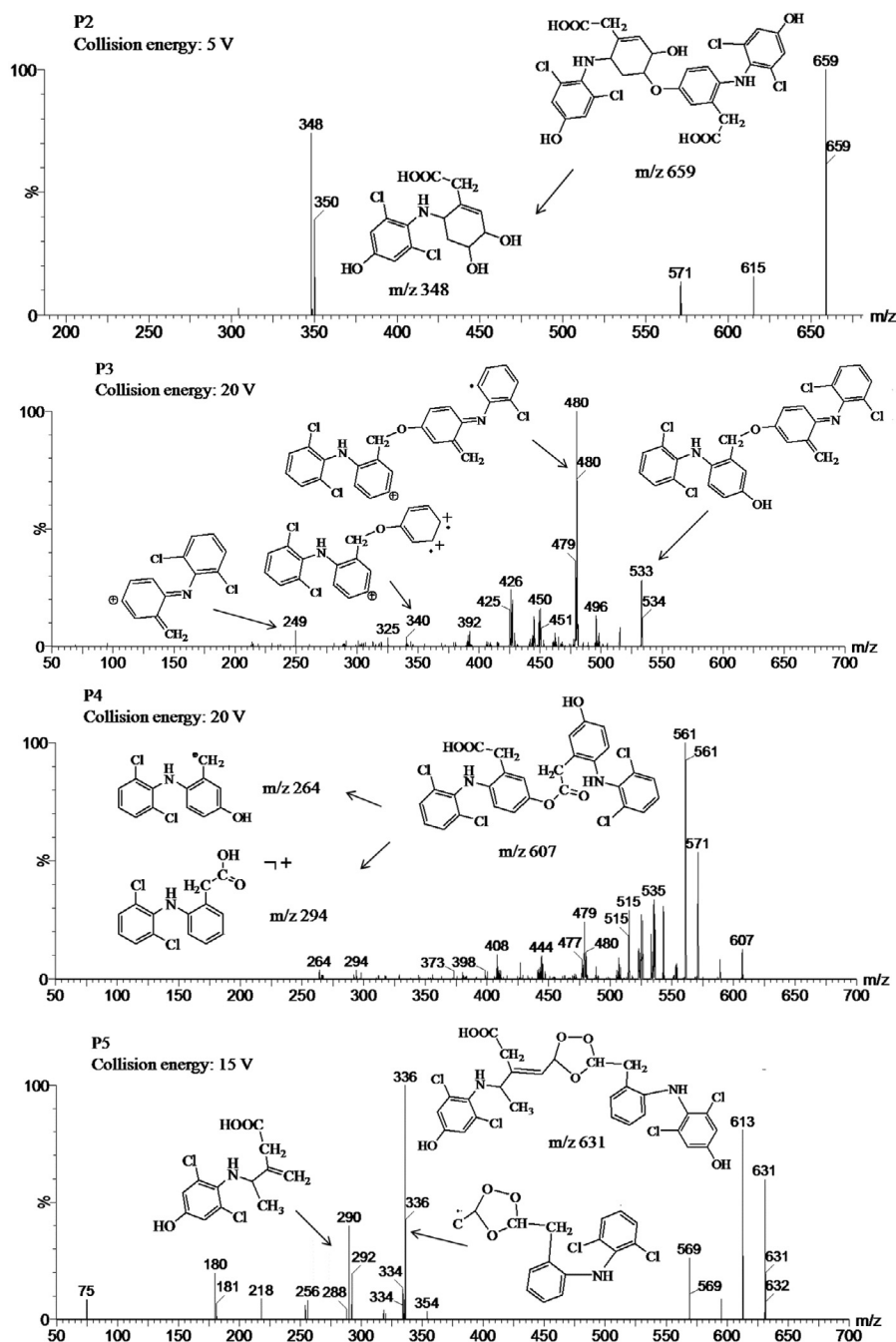
Fig. 3 – MS spectra and proposed structures of oligomeric products (P2: *m/z* 659; P3: *m/z* 533; P4: *m/z* 607; P5: *m/z* 631) for DCF by birnessite.

Mn-O in the MnO_6 octahedral framework (Yang et al. 2007; Händel et al., 2013). Compared with the spectrum of non-reacted birnessite, there was no significant change in the vibration of birnessite backbone that underwent reaction with DCF (Fig. 4b, c). It was indicated that structure of birnessite was not changed, which was consistent with XRD observation (Appendx A Fig. S7).

Moreover, neither the function groups of DCF (*i.e.* 1577 cm^{-1} ($\nu_{as\ COO}$), 1558 cm^{-1} (δ_{N-H}), 1452/1400 cm^{-1} ($\nu_{s\ COO}$), and 1305/1284 cm^{-1} ($\nu_{C-N,\ arom}$)) nor other organic function groups

of products (*i.e.* C=C and C–N) were not observed in birnessite after reacting with DCF (Bucci et al., 1998; Bartolomei et al., 2006). Combined with desorption experiment result **(Appendx A Table S2)**, it was induced that DCF and its transformation products were not adsorbed by birnessite. The oxidation process of DCF by birnessite occurred at the mineral-water interface. DCF and birnessite formed surface complex firstly and then an electron was transferred from the substrate to birnessite (Zhao et al., 2019). Meanwhile, the transformation products of DCF stayed in aqueous phase after reaction.
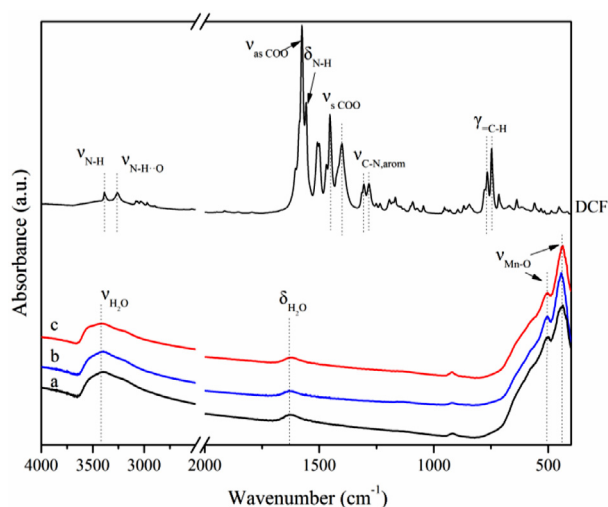
Fig. 4 – FT-IR spectra of DCF and birnessite which was reacted with different initial concentration of DCF ((a) 0 mg/L, (b) 10 mg/L, and (c) 50 mg/L).

2.3.2. Analyses of Mn oxidation state

As shown in Fig. 5a, Mn AOS and the content of Mn(III) for birnessite in the absence of DCF did not change significantly with time increased, while the concentration of Mn(II) increased with reaction time extension. In the presence of DCF, the content of Mn AOS decreased as time course and was significantly lower than that of blank sample in late stage of reaction progress (24, 48 and 72 hr). Meanwhile, the concentration of Mn(III) in birnessite reacting with DCF increased obviously with increasing reaction time. Compared with the content detected from unreacted birnessite-control samples, the decreased in the level of Mn AOS and increased in the level of Mn(III) gave evidence of Mn reduction in reacted birnessite samples. This conclusion was supported by the results of XPS analyses (Fig. 5b-d).

The obtained Mn 3s multiplet splitting values ($\triangle E$) were 4.77 eV for birnessite-control sample, 4.79 eV for birnessite reacted with DCF for 12 hr, and 5.06 eV for birnessite reacted with DCF for 72 hr, respectively (Fig. 5b). The Mn AOS in these samples were 3.60, 3.56 and 3.27 through the relationship AOS = 8.956 – 1.126•$\triangle E$ (**Appendx A Table S3**) (Galakhov et al., 2002; Tu et al., 2014), which was in agreement with the chemical analyses results of Mn AOS. According to the spectral fitting result of XPS Mn 2p (Fig. 5c and d and **Appendx A Table S4**), the Mn(III) content increased from 41.35% in the unreacted sample (t = 0 hr) to 61.16% in the 12 hr reacted birnessite and continued in a systematic manner to 66.39% in the 72 hr reacted sample. And the increase of Mn(III) content was offset by a decrease of Mn(IV) content from 52.61% (0 hr) to 27.22% (72 hr). The reduction of Mn in birnessite suggested that birnessite acted as an oxidant in the reaction process. The reduction of Mn in birnessite suggested that birnessite acted as an oxidant in the reaction process.

As shown in Fig. 5a, the change of Mn(II) in aqueous as time course with the presence of DCF was not significant. And the content of Mn(II) in birnessite reacted with DCF for different time (0, 12 and 72 hr) remained essentially constant at

6.04%-7.09% of the total Mn (Fig. 5d). There might be no Mn(II) formed through reduction of Mn(IV/III) in birnessite during the reaction process. The proportional relationship between increased content of Mn(III) and decreased content of Mn(IV) ($\approx$ 1: 1.01) obtained from XPS analyses confirmed this conclusion. The oxidation of DCF by birnessite was mainly consumed Mn(IV) in birnessite to form Mn(III). Additionally, the concentration of generated Mn(III) (23.84 μmol/L) in birnessite reacting with DCF for 72 hr was lower than the decrease amount of DCF (33.97 μmol/L) in system (Fig. 5a). Considering the formations of four dimers in system, it was reasonable to deduce that the reaction between DCF and birnessite might not only involve in iso-electron transfer reaction from DCF to Mn^{IV}, but also coupling and rearrangement reactions of radical intermediates.

It was worth noting that the concentration of Mn(II) was lower than that observed in birnessite-control system during the whole reaction progress (Fig. 5a). Since no reductant existed in birnessite-control system, the release of Mn(II) was unlikely to be the results of Mn(IV) and/or Mn(III) reduction. The increased in the level of Mn(II) might cause by proton-promoted dissolution of birnessite. H$^+$ attached stepwise to oxygen bridging two metal sites (Mn-O-Mn) and weaken Mn-O bond (Banerjee and Nesbitt, 1999). The addition of DCF inhibited proton-promoted release of dissolved Mn(II) from birnessite into aqueous solution through preventing H$^+$ bridging with oxygen atoms on birnessite solid surface.

2.3.3. Transformation pathways

Based on the product identification discussed above, the changes of Mn valence state in birnessite and the literature about oxidation of DCF by metal oxides and other oxidants, reaction schemes for the oxidation of DCF by birnessite were proposed (Fig. 6). DCF diffused into boundary layer and formed a surface complex on birnessite. Then the electron donating group amine nitrogen of DCF was first attacked to form cation radical, which was also attack site in the process of DCF oxidized by ozone (Sein et al., 2008). One electron was transferred from the radical N to Mn(IV) yielding an iminium ion. Hydroxylation at C5 position of the iminium ion formed intermediate product 5-OH-DCF. Then 5-OH-DCF which possessed a relatively high reaction activity was further transformed to 2,5-IQ-DCF with a quinine-like structure. Hydroxylation process was the major transformation pathway (I) of DCF oxidized by birnessite.

Meanwhile, dimerization process (II) also took place during the reaction (Fig. 6). The formation of four dimers indicated that other unstable intermediates might be formed in current study which could undergo cross-coupling or binding reactions in the presence of birnessite. In fact, not only 5-OH-DCF but also 4'-hydroxydiclofenac and/(or) 4',5-dihydroxydiclofenac could be formed during hydroxylation process of DCF in presence of oxidants due to large reactivity of both C-4' and C-5 carbons of DCF (Chong et al., 2017). Hydroxydiclofenac contained phenolic hydroxyl group could be oxidized by birnessite to form phenoxy radical, which may couple to each other to form polymers (Kang et al., 2004). Considering the observed fragments of P2 in MS/MS spectra, it was formed likely due to the coupling of 4',5-dihydroxydiclofenac. Meanwhile, quinine imine derivative (i.e. 2,5-IQ-DCF) also
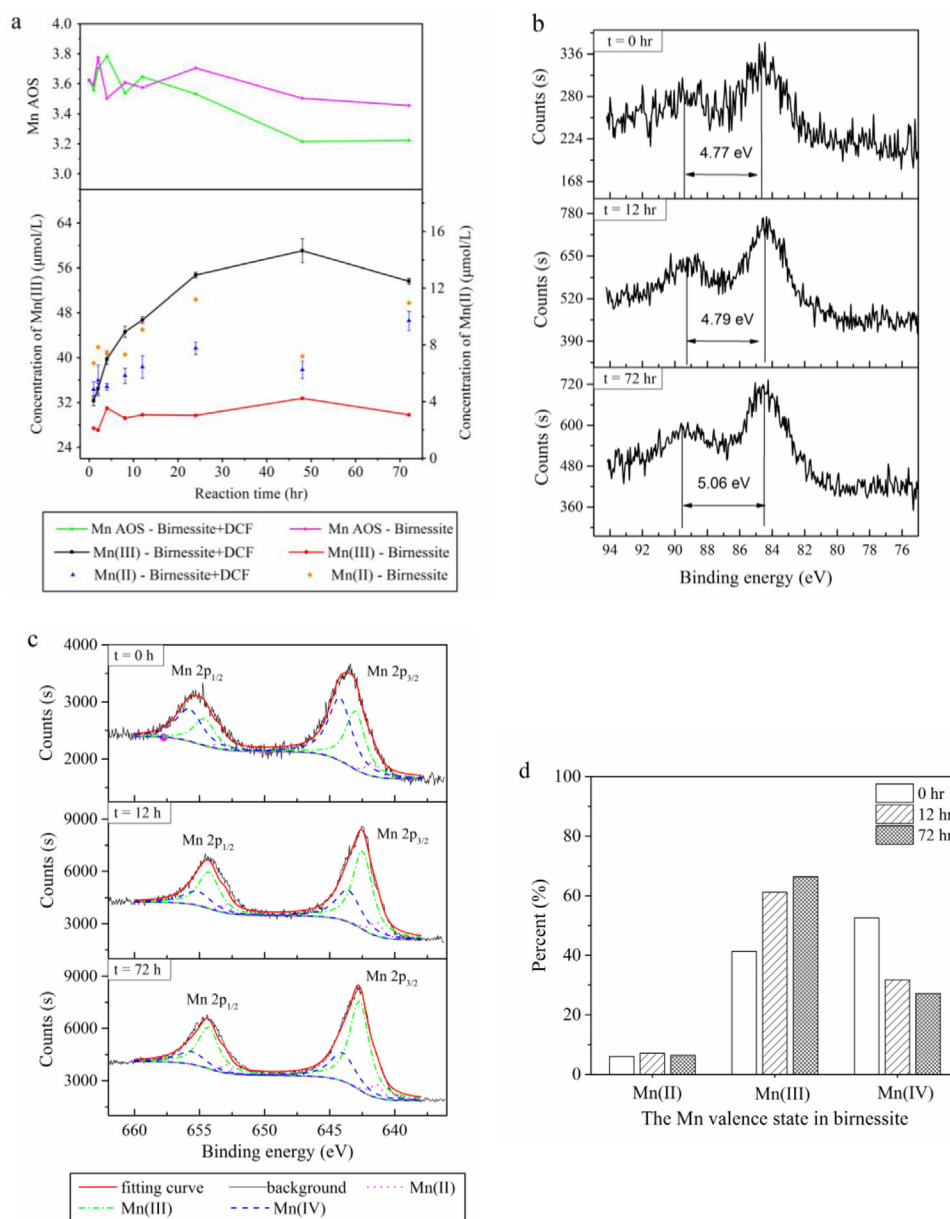
Fig. 5 – Changes of Mn valence in birnessite as time course (a) and XPS spectra of birnessite for different time ((b) XPS spectra in the Mn 3s; (c) XPS spectra in the Mn 2p; (d) proportions of different Mn valence state in birnessite;). Error bars (±1 standard deviation, n = 3) are shown in the figures.

could undergo hydroxylation reaction on the dihalogenated ring with presence of oxidant (Perez-Estrada et al., 2005). Moreover, 2,5-IQ-DCF is not stable, and the C3 = C4 olefin bond may be attacked by oxidants (Lu et al., 2017) and undergo a ring-opening reaction. Therefore, P4 and P5 were formed likely due to the coupling of [6-(2,6-dichloro-4-hydroxy-phenylimino)-3-oxo-cyclohexa-1,4-dienyl]- acetic acid with 5-OH-DCF and 4'-hydroxydiclofenac respectively according to their mass fragments in current study. And ring-opening reaction occurred in the formation of P5. Additionally, as reported in previous study, 2,5-IQ-DCF could undergo decarboxylation reactions in the aliphatic chain which was facilitated by the delocalization of a lone pair at benzylic position in the presence of manganese oxides (Huguet et al., 2013). The decarboxylation pro-

cess of 2,5-IQ-DCF gave rise to an unstable azaquinone methide which would go further to form some different unstable decarboxylated intermediates. In presence of birnessite, unstable decarboxylated intermediates might undergo dimerization and further formed P3 (Fig. 6).

3.   Conclusions

Based on the experimental results in laboratory, reaction mechanism between DCF and birnessite was investigated profoundly and transformation pathways of DCF were proposed. With presence of birnessite, chloride anion was not detected and TOC decreased slightly as reaction progress. It was sup-
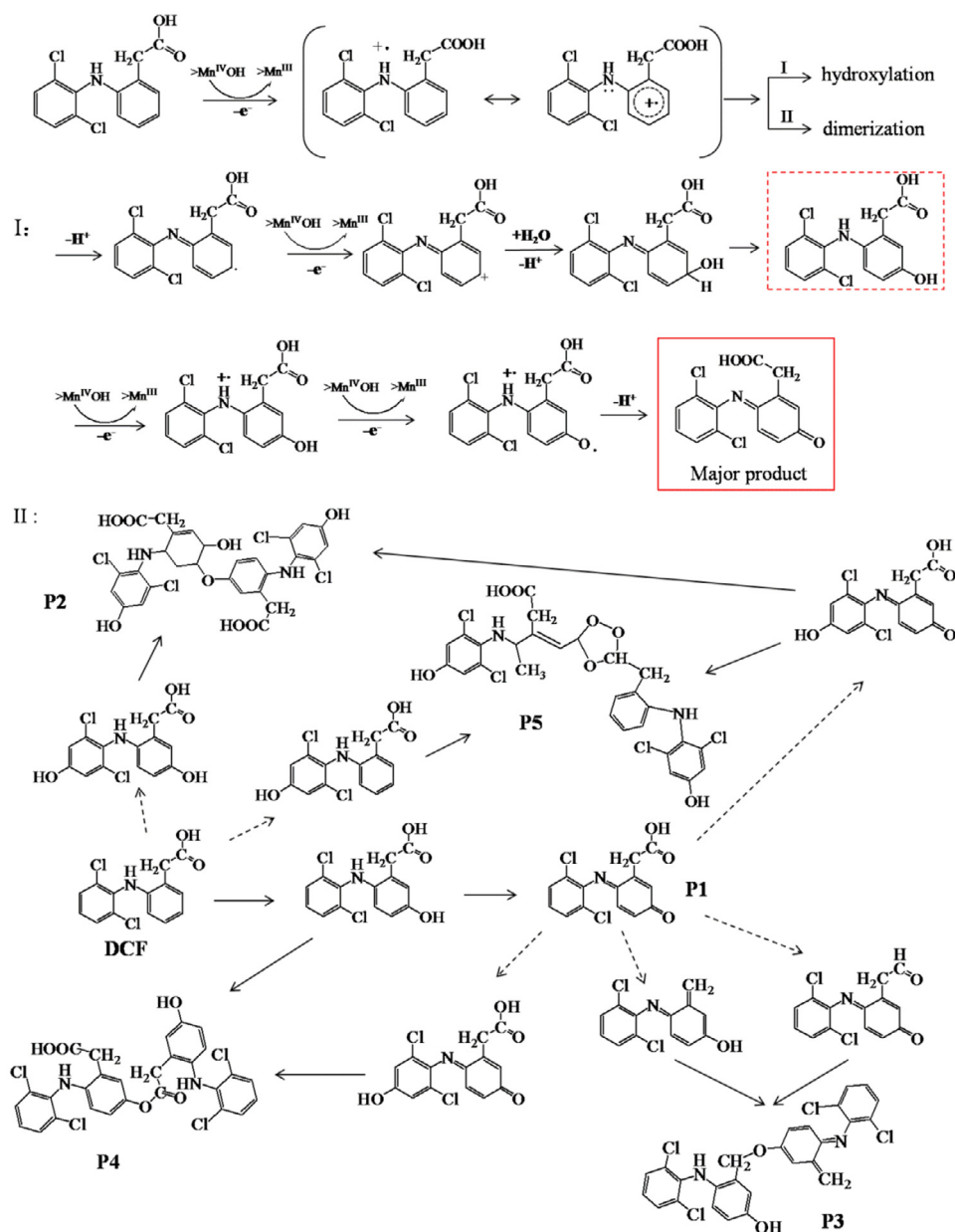
Fig. 6 – Proposed reaction scheme for the oxidation of DCF by birnessite.

ported that the mineralization of DCF was not occurred and DCF was transformed to other organic compounds. Identification of transformation products of DCF proved the presence of hydroxylation and dimerization in reaction process. Hydroxylation process as an iso-electron transfer reaction was the main transformation pathway of DCF reacted with birnessite. 5-OH-DCF was formed via hydroxylation of DCF and further oxidized to form 2,5-IQ-DCF which was identified as a major product accounting for 83.09% of the transformed DCF. Meanwhile, dimerization process as minor transformation pathway of DCF occurred through oxidative-coupling of unstable intermediates in reaction progress. After reaction, the products of DCF were remained in aqueous phase. DCF oxidized by birnessite through consuming the Mn(IV) in birnes-

site structure. Mn(IV) was mainly converted to Mn (III) during the reaction, and Mn(III) was not further converted to Mn(II) finally.

According to the report in other studies, 2,5-IQ-DCF has greater biological toxicity or hepatotoxicity than DCF (Miyamoto et al., 1997; Huber et al., 2016). The content of manganese oxides in soils/sediments is less than 1%, while the concentration of DCF in soils/sediments is in nanogram level. In natural environment, the ratio of birnessite to DCF is about 10^6-10^{10}, which is much higher than the experimental system in this study (100 equiv.). Therefore, DCF in natural soils/sediments is theoretically more likely to react with birnessite to form product 2,5-IQ-DCF. The findings of this work have attracted sufficient attention to warrant future studies.

Acknowledgments

Appendix A Supplementary data

Supplementary material associated with this article can be found, in the online version, at doi:10.1016/j.jes.2020.05.017.

REFERENCES

Acuña, V., Ginebreda, A., Mor, J.R., Petrovic, M., Sabater, S., Sumpter, J., et al., 2015. Balancing the health benefits and environmental risks of pharmaceuticals: Diclofenac as an example. Environ. Int. 85, 327–333.

Agüera, A., Pérez Estrada, L.A., Ferrer, I., Thurman, E.M., Malato, S., Fernández-Alba, A.R., 2005. Application of time-of-flight mass spectrometry to the analysis of phototransformation products of diclofenac in water under natural sunlight. J. Mass Spectrom. 40, 908–915.

Banerjee, D., Nesbitt, H.W., 1999. XPS study of reductive dissolution of birnessite by oxalate: rates and mechanistic aspects of dissolution and redox processes. Geochim. Cosmochim. Acta 63, 3025–3038.

Bartolomei, M., Bertocchi, P., Antoniella, E., Rodomonte, A., 2006. Physico-chemical characterisation and intrinsic dissolution studies of a new hydrate form of diclofenac sodium: comparison with anhydrous form. J. Pharm. Biomed. Anal. 40, 1105–1113.

Biel-Maeso, M., Corada-Fernández, C., Lara-Martín, P.A., 2017. Determining the distribution of pharmaceutically active compounds (PhACs) in soils and sediments by pressurized hot water extraction (PHWE). Chemosphere 185, 1001–1010.

Biel-Maeso, M., Corada-Fernández, C., Lara-Martín, P.A., 2018. Monitoring the occurrence of pharmaceuticals in soils irrigated with reclaimed wastewater. Environ. Pollut. 235, 312–321.

Bucci, R., Magrì, D.A., Magrì, L.A., 1998. Determination of diclofenac salts in pharmaceutical formulations. Fresenius J. Anal. Chem. 362, 577–582.

Chen, B., Gao, Z.Q., Liu, Y., Zheng, Y.M., Han, Y., Zhang, J.P., et al., 2017. Embryo and developmental toxicity of cefazolin sodium impurities in zebrafish. Front. Pharmacol. 8, 403.

Chen, W., Xu, J., Lu, S., Jiao, W., Wu, L., Chang, A.C., 2013. Fates and transport of PPCPs in soil receiving reclaimed water irrigation. Chemosphere 93, 2621–2630.

Cheng, H., Song, D., Liu, H., Qu, J., 2015. Permanganate oxidation of diclofenac: The pH-dependent reaction kinetics and a ring-opening mechanism. Chemosphere 136, 297–304.

Chong, S., Zhang, G., Zhang, N., Liu, Y., Huang, T., Chang, H., 2017. Diclofenac degradation in water by FeCeOₓ catalyzed H₂O₂: Influencing factors, mechanism and pathways. J. Hazard. Mater. 334, 150–159.

Duan, Y.P., Dai, C.M., Zhang, Y.L., Ling, C., 2013. Selective trace enrichment of acidic pharmaceuticals in real water and sediment samples based on solid-phase extraction using multi-templates molecularly imprinted polymers. Anal. Chim. Acta 758, 93–100.

El-Deen, E.Z., El-Mahdy, N., El Rashidy, M., Ghorab, M., Gad, S., Yassin, H., 2016. Diclofenac-induced gastric ulceration in rats: Protective roles of pantoprazole and misoprostol. Br. J. Pharma. Res. Int. 1–12.

Forrez, I., Carballa, M., Verbeken, K., Vanhaecke, L., Schlüsener, M., Ternes, T., et al., 2010. Diclofenac oxidation by biogenic manganese oxides. Environ. Sci. Technol. 44, 3449–3454.

Galakhov, V.R., Demeter, M., Bartkowski, S., Neumann, M., Ovechkina, N.A., Kurmaev, E.Z., et al., 2002. Mn 3s exchange splitting in mixed-valence manganites. Phys. Rev. B 65, 113102.

Groning, J., Held, C., Garten, C., Claussnitzer, U., Kaschabek, S.R., Schlomann, M., 2007. Transformation of diclofenac by the indigenous microflora of river sediments and identification of a major intermediate. Chemosphere 69, 509–516.

Händel, M., Rennert, T., Totsche, K.U., 2013. A simple method to synthesize birnessite at ambient pressure and temperature. Geoderma 193-194, 117–121.

Huber, C., Preis, M., Harvey, P.J., Grosse, S., Letzel, T., Schroder, P., 2016. Emerging pollutants and plants - Metabolic activation of diclofenac by peroxidases. Chemosphere 146, 435–441.

Huguet, M., Deborde, M., Papot, S., Gallard, H., 2013. Oxidative decarboxylation of diclofenac by manganese oxide bed filter. Water Res. 47, 5400–5408.

Kang, K.H., Dec, J., Park, H., Bollag, J.M., 2004. Effect of phenolic mediators and humic acid on cyprodinil transformation in presence of birnessite. Water Res. 38, 2737–2745.

Kijima, N., Yasuda, H., Sato, T., Yoshimura, Y., 2001. Preparation and characterization of open tunnel oxide α-MnO₂ precipitated by ozone oxidation. J. Solid State Chem. 159, 94–102.

Klewicki, J.K., Morgan, J.J., 1998. Kinetic behavior of Mn(III) complexes of pyrophosphate, EDTA, and citrate. Environ. Sci. Technol. 32, 2916–2922.

Li, L., Wei, D., Wei, G., Du, Y., 2017. Product identification and the mechanisms involved in the transformation of cefazolin by birnessite (δ-MnO₂). Chem. Eng. J. 320, 116–123.

Lindholm-Lehto, P.C., Ahkola, H.S., Knuutinen, J.S., Herve, S.H., 2015. Occurrence of pharmaceuticals in municipal wastewater, in the recipient water, and sedimented particles of northern Lake Päijänne. Environ. Sci. Pollut. Res. 22, 17209–17223.

Lu, X., Shao, Y., Gao, N., Chen, J., Zhang, Y., Xiang, H., et al., 2017. Degradation of diclofenac by UV-activated persulfate process: Kinetic studies, degradation pathways and toxicity assessments. Ecotoxicol. Environ. Saf. 141, 139–147.

Lu, Z., Lin, K., Gan, J., 2011. Oxidation of bisphenol F (BPF) by manganese dioxide. Environ. Pollut. 159, 2546–2551.

McKenzie, R.M., 1971. The synthesis of birnessite, cryptomelane, and some other oxides and hydroxides of manganese. Mineral. Mag. 38, 493–502.

Meyer, W., Reich, M., Beier, S., Behrendt, J., Gulyas, H., Otterpohl, R., 2016. Measured and predicted environmental concentrations of carbamazepine, diclofenac, and metoprolol in small and medium rivers in northern Germany. Environ. Monit. Assess. 188, 487.

Miyamoto, G., Zahid, N., Uetrecht, J.P., 1997. Oxidation of diclofenac to reactive intermediates by neutrophils, myeloperoxidase, and hypochlorous acid. Chem. Res. Toxicol. 10, 414–419.

Oaks, J.L., Gilbert, M., Virani, M.Z., Watson, R.T., Meteyer, C.U., Rideout, B.A., et al., 2004. Diclofenac residues as the cause of vulture population decline in Pakistan. Nature 427, 630–633.

Perez-Estrada, L.A., Malato, S., Gernjak, W., Aguera, A., Thurman, E.M., Ferrer, I., et al., 2005. Photo-fenton degradation of diclofenac: identification of main intermediates and degradation pathway. Environ. Sci. Technol. 39, 8300–8306.

Qin, M.G., Zhao, H.L., Yang, W.J., Zhou, Y.R., Li, F., 2016. A facile one-pot synthesis of three-dimensional microflower birnessite (delta-MnO₂) and its efficient oxidative degradation of rhodamine B. RSC Adv. 6, 23905–23912.

Rede, D., Santos, L., Ramos, S., Oliva-Teles, F., Antao, C., Sousa, S.R., et al., 2019. Individual and mixture toxicity evaluation of three pharmaceuticals to the germination and growth of Lactuca sativa seeds. Sci. Total Environ. 673, 102–109.

Sein, M.M., Zedda, M., Tuerk, J., Schmidt, T.C., Golloch, A., Sonntag, C.V., 2008. Oxidation of diclofenac with ozone in aqueous solution. Environ. Sci. Technol. 42, 6656–6662.

Simazaki, D., Kubota, R., Suzuki, T., Akiba, M., Nishimura, T., Kunikane, S., 2015. Occurrence of selected pharmaceuticals at drinking water purification plants in Japan and implications for human health. Water Res. 76, 187–200.

Tu, J., Yang, Z., Hu, C., Qu, J., 2014. Characterization and reactivity of biogenic manganese oxides for ciprofloxacin oxidation. J. Environ. Sci. 26, 1154–1161.

Wang, J., Wang, S., 2016. Removal of pharmaceuticals and personal care products (PPCPs) from wastewater: a review. J. Environ. Manage. 182, 620–640.

Wang, L., Cheng, H., 2015. Birnessite (δ-MnO₂) mediated degradation of organoarsenic feed additive p-Arsanilic acid. Environ. Sci. Technol. 49, 3473–3481.

Wang, Y., Liu, H, Xie, Y, Ni, T., Liu, G., 2015. Oxidative removal of diclofenac by chlorine dioxide: Reaction kinetics and mechanism. Chem. Eng. J. 279, 409–415.

Webb, S.M., Dick, G.J., Bargar, J.R., Tebo, B.M., 2005. Evidence for the presence of Mn(III) intermediates in the bacterial oxidation of Mn(II). Proceedings of the National Academy of Sciences of the United States of America 102 (15), 5558–5563.

Xu, J., Wu, L., Chang, A.C., 2009. Degradation and adsorption of selected pharmaceuticals and personal care products (PPCPs) in agricultural soils. Chemosphere 77, 1299–1305.

Yang, L., Lan, W., Pan, B., Chao, W., Shuang, B., Nie, X., 2017. Toxic effects of diclofenac on life history parameters and the expression of detoxification-related genes in Daphnia magna. Aquat. Toxicol. 183, 104–113.

Yang, L.X., Zhu, Y.J., Cheng, G.F., 2007. Synthesis of well-crystallized birnessite using ethylene glycol as a reducing reagent. Mater. Res. Bull. 42, 159–164.

Zhao, W., Feng, X., Tan, W., Liu, F., Ding, S., 2009. Relation of lead adsorption on birnessites with different average oxidation states of manganese and release of Mn²⁺/H⁺/K⁺. J. Environ. Sci. 21, 520–526.

Zhao, Y., Liu, F., Qin, X., 2017. Adsorption of diclofenac onto goethite: Adsorption kinetics and effects of pH. Chemosphere 180, 373–378.

Zhao, Y., Liu, F., Qin, X., 2019. Removal of diclofenac from aqueous phase by birnessite: Effects of pH and common ions. Water, Air, Soil Pollut. 230, 14.